Combined Texture Analysis of MR images and Glypican-3 to Identify the Differentiated Degree of Hepatocellular Carcinoma: a retrospective study

Mengmeng Feng
first affiliated hospital of soochow university
Mengchao Zhang
China-Japan Union Hospital of Jilin University
Yuanqing Liu
First Affiliated Hospital of Soochow University
Nan Jiang
First Affiliated Hospital of Soochow University
Qian Meng
First Affiliated Hospital of Soochow University
Jia Wang
First Affiliated Hospital of Soochow University
Ziyun Yao
First Affiliated Hospital of Soochow University
Hui Dai (huizi198208@126.com)
https://orcid.org/0000-0001-5024-559X

Research article

Keywords: hepatocellular carcinoma, differentiated degree, texture feature, glypican-3

Posted Date: March 11th, 2020

DOI: https://doi.org/10.21203/rs.3.rs-16860/v1

Version of Record: A version of this preprint was published on June 30th, 2020. See the published version at https://doi.org/10.1186/s12885-020-07094-8.

Combined Texture Analysis of MR images and Glypican-3 to Identify the Differentiated Degree of Hepatocellular Carcinoma: a retrospective study

Mengmeng Feng[#1], Mengchao Zhang[#2], Yuanqing Liu[1], Nan Jiang[1], Qian Meng[1], Jia Wang[3]，Ziyun Yao[4]，Hui Dai[*1,5]

1 Department of Radiology, the First Affiliated Hospital of Soochow University, Suzhou city, Jiangsu province, P.R.China 215000

2 Department of Radiology, the China-Japan Union Hospital of Jilin University, Changchun city, Jilin province, P.R. China 130033

3 Department of Hepatobiliary surgery department, the First Affiliated Hospital of Soochow University, Suzhou city, Jiangsu province, P.R.China 215000

4 Department of Pathology department, the First Affiliated Hospital of Soochow University, Suzhou city, Jiangsu province, P.R.China 215000

5 Institute of Medical Imaging, Soochow University, Suzhou city, Jiangsu province, P.R.China 215000

[#] These authors contributed equally to this work.

Mengmeng Feng 18375338426@163.com
Mengchao Zhang zhangmengchao@jlu.edu.cn
Yuanqing Liu 18895686921@163.com
Nan Jiang 519033749@qq.com
Qian Meng qianmengmq@163.com
Jia Wang 15862417362@163.com
Ziyun Yao yzy677196@163.com

Corresponding Author

Hui Dai Ph.D.

e-mail: huizi198208@126.com

telephone number: 0512-67780633

fax number: 0512-67780633

correspondence address: Department of Radiology, The First Affiliated Hospital of Soochow University, Suzhou, Jiangsu, P.R.China 215000

Abstract

BACKGROUD

To explore the clinical value of texture analysis of MR images (multiphase Gd-EOB-DTPA-enhanced MRI and T2 weighted imaging (T2WI) and the glypican-3 (GPC-3) to identify the differentiated degree of hepatocellular carcinoma (HCC).

METHOD

In this retrospective study, 104 participants were enrolled (GPC-3 data obtained in 51 participants). Each participant performed preoperative Gd-EOB-DTPA-enhanced MR scanning. Texture analysis was calculated by MaZda and then using the B11 program for data analysis and classification. The performance of texture features and GPC-3 in identifying the differentiated degree of HCC was assessed by receiver operating characteristic (ROC) analysis.

RESULTS

There were no statistically significances for the expression of GPC-3 between poorly-, well- and moderately-differentiated HCC. The area under the curve (AUC) of the combined texture features between poorly- and well-differentiated HCC, poorly- and moderately-differentiated HCC, moderately- and well-differentiated HCC was 0.812, 0.879 and 0.808 respectively. With GPC-3 combined, the AUC was increased to 0.868, while accuracy was decreased, in poorly- verse well-differentiated HCC, and the AUC and accuracy were the same as those without GPC-3 combined in poorly- verse moderately-differentiated HCC. Although the AUC was increased to 0.818 with GPC-3 combined in moderately- verse well-differentiated HCC, there were no statistical significance for the value change ($p>0.05$).

CONCLUSIONS

Texture analysis of Gd-EOB-DTPA-enhanced MRI and T2WI are valuable in identifying the differentiated degree of HCC. There is no significant effect of GPC-3 in identifying the differentiated degree of HCC, suggesting the promising value of texture analysis of MR images in the precise presurgical diagnosis of HCC.

Keywords: hepatocellular carcinoma, differentiated degree, texture feature, glypican-3

BACKGROUD

Hepatocellular carcinoma (HCC) is a malignant tumor evolved from the hepatocyte and is the second most common cause of cancer death worldwide. HCC account for a larger proportion of tumor particularly in developing countries[1]. The high prevalence of hepatitis virus B is the most common reason leading to HCC in the developing countries, while the alcohol and hepatitis C virus is more frequent in developed

countries. Although there are many treatments of HCC including surgery, radiofrequency ablation and transcatheter arterial chemoembolization (TACE), the mortality of HCC is still high due to the recurrence[2].

There were many reports suggested that the size of tumor, number of lesion, vascular invasion, status of tumor capsule and liver function status can affect the prognosis and the choices of therapy of HCC[3-6]. Nevertheless, the most important factor was the differentiated grade, which was supposed to an independent factor affecting recurrence of HCC[7]. According to the differentiated degree of tumor cells, HCC were grouped into poorly-differentiated HCC, moderately-differentiated HCC and well-differentiated HCC. According to the reports, the overall survival rate of the patients with moderately-differentiated and well-differentiated HCC was higher than that of the patients with poorly-differentiated HCC, while the recurrence rate was lower[8, 9].

As we known, a precise pre-surgical evaluation of differentiated degree of HCC might affect the individual treatment schedule[10]. Currently, aspiration biopsy was the most common method to get the information of histopathology before surgery. However, it was criticized by many researchers due to its invasiveness and the probability of seeding metastasis[11, 12]. Recently, many studies suggested the image characteristics of tumor might predict the differential degree of the HCC. For example, there were some reports found that the low density/intensity of HCC on the portal phase of CT and hepatobiliary phase of Gd-EOB-DTPA-enhanced MRI might help to identify the differentiated degree of HCC[13, 14].

Glypican-3 (GPC-3), a special marker of HCC, has been used to identify the HCC from other tumors and to evaluate the prognosis. GPC-3 is a member of the glypican family, which influences cell growth, differentiation, and migration[15]. GPC-3 is highly expressed in HCC, but not in cholangiocarcinoma or normal hepatic cells and is low express in well differential HCC[16, 17]. Previous studies have shown that higher

GPC-3 expression level in HCC is a risk factor for shorter overall survival (OS) and levels of GPC-3 expression in poorly-differentiated tumor cells were higher than moderately- and well- differentiated HCC[15, 18].

Texture analysis was an established technique，which was beneficial to diagnoses, by extracting a large amount of texture information from medical images[19]. Until now, texture analyses have been used in identifying the differentiated degree and characteristics of tumor, evaluating the therapeutic effect, etc[20-22].

To the authors' knowledge, the texture analyses have not been used in identifying the differentiated degree of HCC yet. Thus, our aim of the present study is to evaluate the accuracy of the texture analysis of MR images and the effect of GPC-3 in discriminating the differentiated degree of HCC.

Materials and methods

Patients

The present study received ethical approval from the Medical Ethics Review Committee of our institution and the relevant informed consent form was obtained in accordance with the Declaration of Helsinki. 104 participants were enrolled from 2015 to 2019, according to the following criteria:1) pathologically proved as HCC after hepatectomy or aspiration biopsy; 2) inpatients who have comprehensive clinic materials; 3) performed preoperative Gd-EOB-DTPA-enhanced MRI. The clinic data of the 104 participants were recorded in the Table 1, containing age, gender, alpha fetoprotein (AFP), alamine aminotransferase (ALT), aspartate transaminase (AST), ALT\AST, total bilirubin (TBIL), direct bilirubin and indirect bilirubin. The histopathlogical data of GPC-3 was obtained in 51 participants.

Exclusion criteria included:1) participants have been treated (transplantation, resection, ablation or embolization) before MR examination;

2) clinical data or pathological results were incomplete; 3) the lesions were not clearly displayed on the images due to the artifact.

MRI examination

All MRI examinations were performed using a 3 T MRI machine (MAGNETOM Verio; SKYRA; signa, GE) with a dedicated phased-array body coil. A standard abdominal MRI protocol containing following sequences were acquired: 1) Axial T2-weighted : TR=3260ms, TE=105ms, slice thickness 7 mm, intersection gap 1.4 mm, field of view (FOV) 210mm×380mm; 2) In-phase and out-of-phase axial T1-weighted imaging: TR=4.16ms, TE=2.58ms (in-phase), TE=1.35ms (out-phase), slice thickness 5 mm, intersection gap 1 mm, FOV 210mm×380mm; 3) Diffusion-weighted imaging (DWI, b=50, 800 s/mm^2) performed with a free-breathing single-shot echo-planar technique, TR 5300ms, TE 57ms, slice thickness 7 mm, intersection gap 1.4 mm, FOV 210mm×380mm; corresponding ADC maps were calculated automatically by a built-in software; and 4) Contrast enhanced MRI, a three-dimensional (3D) gradient echo sequence with volumetric interpolated breath-hold examination (VIBE): TR 4.18ms, TE 1.93ms, slice thickness 3 mm without intersection gap, FOV 210mm×380mm. Gd-EOB-DTPA (Primovist, Bayer Healthcare, Berlin, Germany) was used by 0.2 ml/kg with an injection rate of 2 ml/sec. Hepatic arterial phase (AP), portal venous phase (PVP), equilibrium phase (EP) and hepatobiliary phase (HBP) images were obtained.

Image analysis

The MRI images were reviewed in the picture archiving and communication system (PACS). Experienced radiologists, who were blinded to the pathological results, evaluated the MRI imaging features of the HCC. The imaging features of MRI (arterial enhancement, capsule appearance, the intensity of HBP， the margin and diameter of tumor, intra-lesion fat, intra-tumor vessel and etc.) were selected referring to the

Liver Imaging-Reporting and Data System (LI-RADS 2017) (https://www.acr.org/Clinical-Resources/Reporting-and-Data-Systems/LI-RADS)[23].

Texture analyses and features selection

MaZda software (version 4.6, quantitative texture analysis software, available from http://www.eletel.p.lodz.pl/mazda/) was used for texture analysis. All images were transformed into Bitmap (BMP) format considering for the application compatibility of MaZda. An experienced radiologist manually portrayed the region of interest (ROI) of the lesion on the slice which contained the maximum proportion of tumor. 104 ROIs (one ROI for each patient) on HBP images were analyzed firstly. Subsequently, the ROIs were copied onto T2, AP and EP images. Then, texture features were extracted and analyzed. Finally, the texture features were grouped into grey-level histogram, the grey-level co-occurrence matrix (GLCOM), the grey-level run-length matrix (GLRLM) and wavelet transform. More detailed texture features are listed in Table 2. Feature selection algorithms included Fisher coefficient, mutual information [MI], and classification error probability combined with average correlation coefficients [POE + ACC]. 10 texture features were extracted by each of these algorithms. In order to enhance the discriminability, these three methods were combined, called “FPM”, by which 30 texture features were extracted in total.

Histopathological analysis

Histopathological evaluation was available after hepatectomy or aspiration biopsy for the lesions. The specimens were routinely prepared with 4% formaldehyde. The specimens were evaluated by two experienced pathologists who were blind to MRI information. The eight slices of each lesion were analyzed and evaluated with slices ranging from 0.3 cm to 2.0 cm depending on the size of the lesion. The Edmonson method was

used to categorize all the specimens. According to the differentiation degree of tumor cells, HCC were categorized into grades I to IV. Grades I and II were defined as well-differentiated HCC, grade III was defined as moderately-differentiated HCC, and grade IV was defined as poorly-differentiated HCC. The specimens were stained with GPC-3 antibodies. The results of immunohistochemical staining were considered positive if more than 10% of the tumor cells showed cytoplasmic staining, otherwise the results were considered negative.

Statistical analysis and misclassification rate

The statistical analysis was performed using Statistical Product and Service Software (SPSS ver. 20.0, Chicago, IL). In present study, the continuous variables which are abnormal distribution, such as age, ALT, AST, ALT\AST and texture features, were compared with Mann-Whitney U test. Categorical variables were compared using Pearson Test when the sample size is over 40 and the minimal expected frequency is over 5. Otherwise, the correction formula of chi-squared test will be chosen. And the R×C table was used when the dependent variable is over 2. The value of $p<0.05$ were considered statistically significant. And Bonferroni correction was used to adjust *P* values. In order to evaluate the diagnostic accuracy of texture features derived from T2, HBP, AP, and EP, the ROC analyses were performed and the area under the curve (AUC) were calculated by MedCalc (MedCalc statistical software, ver.15.8).

The B11, a module of MaZda (version 4.6), provides following four pathways, Principal component analysis (PCA), linear discriminant analysis (LDA), nonlinear discriminant analysis (NDA) and Raw data analysis (RDA), to classify and analyze the texture features. The b11 implements 1-NN classifier for non-linear supervised classification[24]. The misclassification rate is defined as total false samples divided by the total samples and the ratio indicates that the estimated group is different from the observed group. According to the misclassification rate, the

classification results were separate into four levels: excellent (misclassification rates ≤10%), good (10% <misclassification rates ≤20%), moderate (20% <misclassification rates ≤30%), fair (30% <misclassification rates ≤40%), and poor (misclassification rates >40%)[25].

RESULTS

Clinical data

There were 37 patients with poorly-differentiated HCC, 43 with moderately-differentiated HCC, and 24 with well-differentiated HCC in present study. As showed in Table 1, there were no significant differences for age and gender among the groups (p>0.05). There were significant differences for AFP and ALT value between the poor- and well-differentiated HCC (p=0.001, 0.006, respectively). The ALT was statistically different between well- and moderately-differentiated HCC (p=0.008). 51 participants were with GPC-3, among which, 20 were with poorly-differentiated HCC, 20 with moderately and 11 with well-differentiated HCC.

There were no statistical significances for expression of GPC-3 between poorly-, well- and moderately-differentiated HCC, as Table 1 showed.

MRI feature evaluation

The MRI imaging features of l04 patients are demonstrated in Table 3. As the table showed, the tumor size were statistically different between poorly- and moderately-HCC, with p=0.014（p<0.017）. However, no statistical difference in the margin of tumor, the status of tumor's capsule and liver cirrhosis, the HBP hypointensity, intratumoral vessel, intralesion fat, rim-enhancement AP and lymphadenectasis, between poorly-, moderately- and well-differentiated HCC.

Texture analysis and tissue classification

As showed in Table 4, 262 texture features derived from T2, HBP, AP and EP images were obtained and categorized into histogram (n=10), GLCOM (n=220), GLRLM (n=20) and wavelet transform (n=12)[26]. The frequency of each feature category extracted by FPM were showed for T2-weighted images and each phase of Gd-EOB-DTPA enhanced images among poorly-differentiated, well-differentiated and moderately-differentiated HCC. The GLCOM-based texture features were most frequently extracted with three phases for poorly- verse well-differentiated HCC, poorly- verse moderately-differentiated HCC and well- verse moderately-differentiated HCC.

The tissue classification results were demonstrated across the T2, AP, EP and HBP in Table 5. The misclassification rate of NDA was excellent for each phase of the three groups, with the miscalssification rate ranging from 3.33% to 14.93%. The misclassification rate of LDA was rank secondly to NDA, with the classification rate range from 4.92% to 33.75%. Both of the mislassification results of RDA and PCA were fair or poor. The phase of enhanced- MRI may be an important factor which can impact the classification rate of texture analysis when compared poorly-, moderately- and well-differentiated HCC.

ROC-analysis

All of the AUC of the statistically significant texture features were calculated. The ROC curves of the best combined diagnoses were demonstrated in Figure 1-3. As showed in Figure 1, the combine AUC value (combining texture features from T2, AP and EP) was 0.812, higher than that of any single texture feature from each phase, to differentiate poorly- from well-differentiated HCC (accuracy=0.77). As showed in Figure 2, the combine AUC value was 0.879 (accuracy=0.85), to differentiate poorly- from moderately-differentiated HCC, and as showed in Figure 3, the combined AUC value was 0.808 (accuracy=0.746) to differentiate moderately- from well-differentiated HCC.

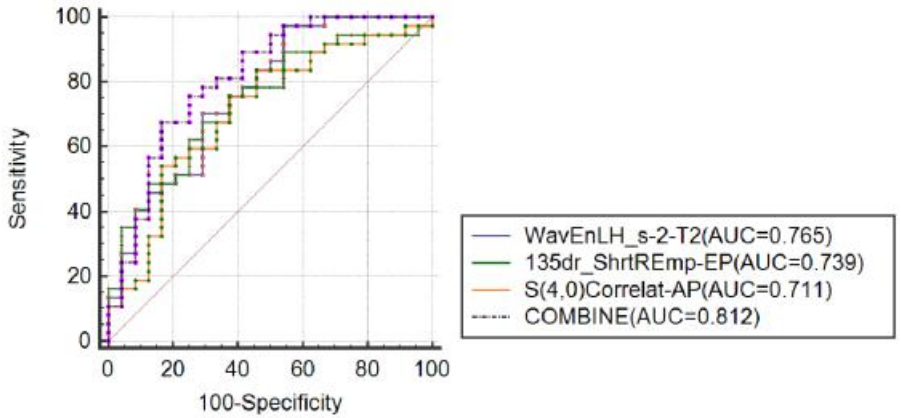

Figure 1 ROC for differentiating the poorly- and well-differentiated HCC. The ROC curves were draw according to the texture features with the highest AUC derived from T2, EP and AP. And the ROC of the combined texture features was also draw as COMBINE.

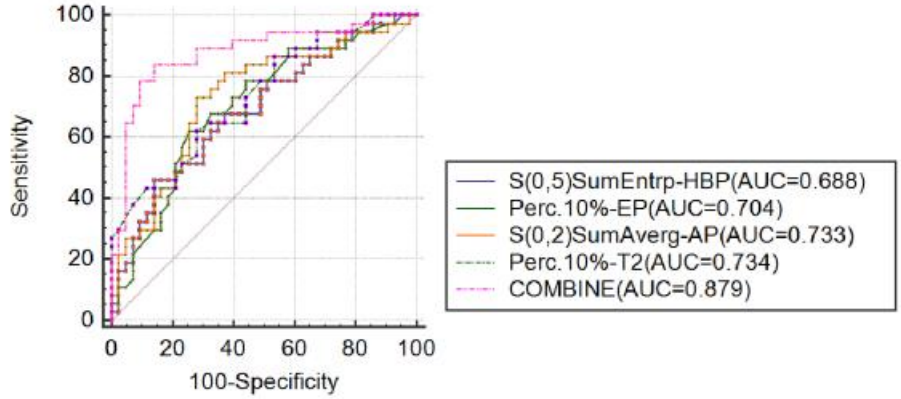

Figure 2 ROC for differentiating the poorly- and moderately-differentiated HCC. The ROC curves were draw according to the texture features with the highest AUC derived from T2, AP, EP and HBP. And the ROC of the combined texture features was also draw as Combine.

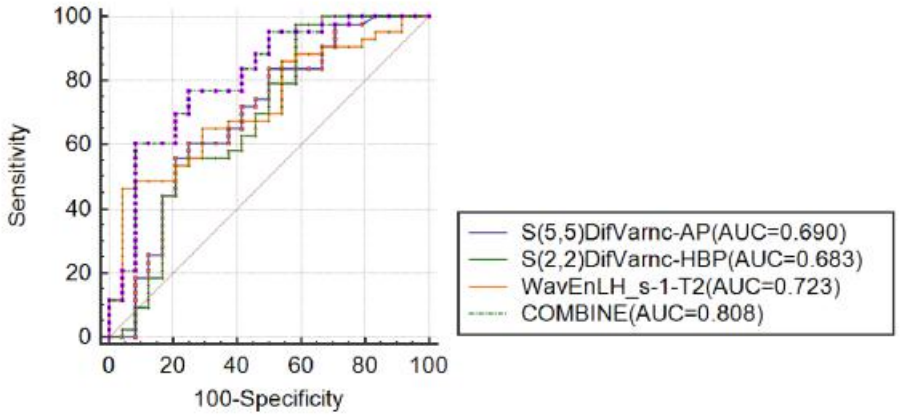

Figure 3 ROC for differentiating the well- and moderately-differentiated HCC. The ROC curves were draw according to the texture features with the highest AUC derived from T2, AP and HBP. And the ROC of the combined texture features was also draw as Combine.

The ROC analyses of combined GPC-3 and texture analyses were demonstrated in Table 6. “COMBINE” presents the combination of texture features derived from different phases. As showed in Table 6, the COMBINE AUC value was higher than that of any single texture feature from each phase. Additionally, the AUC value of combined GPC-3 and texture analyses was increased from 0.818 to 0.868 while the accuracy was decreased, when compared poorly- with well-differentiated HCC. The AUC and accuracy of combined GPC-3 and COMBINE was the same as those of COMBINE AUC (AUC 0.880, accuracy 0.800), in poorly- verse moderately-differentiated HCC. When moderately- verse well-differentiated HCC， the AUC was increased from 0.777 to 0.818 with GPC-3 combined, but there were no statistical significance for the value change (p=0.508).

DISCUSSIONS

As previous studies showed, the diameter of HCC was an important factor to predict the pathological grade of HCC. Lee et al[26] and Martins et al[27] suggested that the diameter of most moderately-differentiated HCC was larger than well-differentiated HCC. Our present study also proved the opinion that the diameter of poorly-differentiated HCC was larger than that of moderately-differentiated and well-differentiated HCC. However, there was no statistical difference of diameter between poorly and well-differentiated HCC in present study, which was not in consistence with the Martins'. Such differences may be due to the heterogeneity of tumor cells themselves and individual differences of tumor growing pattern, as well as the limited sample size.

The differential degree of HCC is the most important factor that affect the prognosis of the patients. In this study, the patients were grouped into poorly, moderately and well-differentiated group based on the histopathological grade and explored whether the texture features can successfully differentiate the subtypes of HCC. Texture analysis is a method that can quantize the information provided by the images. Some studies verified that texture analysis had the potential to identify the histopathological type of neoplasm, such as the breast cancer and renal tumor[25, 28]. However, there are no researches yet to explore the value of texture features derived from mlutiphase of Gd-EOB-DTPA-enhanced MRI and T2WI in predicting the histopathological grades of HCC.

In recent years, researchers gradually realized that the substantial quantitative features was increasingly important in the tumor diagnoses, not merely the application of qualitative features such as margin, signal intensity, capsule of the tumor and so on[29]. Mazda is a software package which provides a complete path for quantitative analysis of image texture. It includes image analysis, texture features extraction, data classification, analysis automation and other functions[24]. Substantial information obtained by Mazda, might differentiate the pathological

grade of tumor. Previous study analyzed the texture features to predict the OS of the patients with advanced HCC[30]. Our study attempted to identify the histopathological grade by texture analysis.

B11 module provides four procedures, RDA, PCA, LDA and NDA, to analyze the selected thirty features. In present study, the classification rate of NDA was excellent. It suggested that texture analysis was a reliable method to identify the poorly-, moderately- and well-differentiated HCC. Although LDA was recommended as an optical method, NDA was demonstrated much preciser than LDA in present study, which was in consistent with Li Y's study[31]. This may due to the non-linearity of the clinical data which was obtained in a random way. And the inconformity of the misclassification rate from the texture analysis of different image sequences, may result from the different histological components and enhancement patterns among the subtypes of HCC[25].

The GLCOM-based features which describe the spatial dependence of gray value in image were most frequently extracted than other texture features of other categories regardless of the phase of MRI and groups[31, 32]. It may imply that the different pathological grade can impact the gray value of the image. But it also may be caused by the tremendous number of GLCOM (n=220)[25]. Besides, the texture features of GLRLM is secondly selected by texture analysis which demonstrates the pixel runs with the same grey level values in a given direction and depicts intensity homogeneity in given direction[31]. The result may depict that the intensity homogeneity between poorly-, moderately- and well-differentiated HCC is different.

The GLCOM-based features generated from AP was noticeably different between groups. As previous study showed, HCC with a higher differentiated degree was prone to have lower arterial supply. The arterial supply differences may lead to the differences of texture features derived from AP[33]. The Correlat depicts the similarity of gray value between the adjacent pixels in the horizontal and vertical directions and

the SumAverg indicates the average gray value of the pixels and reflects the degree of brightness of the image. Our findings suggested that the signal intensity of poorly-differentiated HCC was slightly higher than that of well-differentiated HCC on AP images, which was somewhat approved the abundant arterial supply of poorly-differentiated HCC.

As previous studies showed, GPC-3 was hardly expressed in most of the tissues. However, GPC-3 was a reliable mark of HCC[34, 35]. There were some studies suggested that the expression of GPC-3 of poorly-differentiated HCC was higher than well- and moderately-differentiated HCC and the OS was shorter[16, 17]. But there was no statistical significance of the expression of GPC-3 between poorly-, moderately- and well- differentiated HCC in present study. The small sample size was supposed to be the reason of this discrepancy. Additionally, as showed in Table 6, the diagnosis effect was not improved with the combination of GPC-3 and texture features. It suggested that the texture analysis was a promising and reliable method in identifying the differentiated degree of HCC, even without GPC-3, an index from pathological tissue.

There were some limitations in our study. Although we adopted strict inclusion and exclusion criteria in this retrospective study, selection bias was still inevitably. Second, the sample size was relatively small which need to be enlarged in the future study. Third, the ROI (tumor contour) was manually delineated on the slice containing the maximum diameter, which led to the lack of the 3D information of the tumor. However, the 3D information of the HCC rarely impacted our clinical diagnosis.

In conclusion, the texture analysis of multiphase Gd-EOB-DTPA-enhanced MRI and T2WI are noninvasive and reliable quantitative technique to differentiate the subtypes of HCC. There is no significant effect of GPC-3 in identifying the differentiated degree of HCC, suggesting the promising value of texture analyses of MR images in the precise presurgical diagnosis of HCC.

Abbreviations

HCC, Hepatocellular carcinoma; TACE, transcatheter arterial chemoembolization; GPC-3, Glypican-3; OS, overall survival; AFP, alpha fetoprotein; ALT, alamine aminotransferase; AST, aspartate transaminase; T2WI, T2 weighted imaging; ROC, receiver operating characteristic; AUC, area under the curve; TBIL, total bilirubin; AP, Hepatic arterial phase; PVP, portal venous phase; EP, equilibrium phase; HBP, hepatobiliary phase; ROI, region of interest; GLCOM, the grey-level co-occurrence matrix; GLRLM, the grey-level run-length matrix; PCA, Principal component analysis; LDA, linear discriminant analysis; NDA, nonlinear discriminant analysis; RDA, Raw data analysis.

Declaration

1、The present study received ethical approval from the Medical Ethics Review Committee of our institution and the relevant informed consent form was obtained in accordance with the Declaration of Helsinki.

2、Not applicable consent for publication.

3、The datasets analysed during the current study are available from the corresponding author on reasonable request.

4、Authors declare no conflicts of interest.

5、This work was mainly supported by the National Natural Science Foundation of China (grant number 81971573), and partially supported by the Project of Invigorating Health Care through Science, Technology and Education, Jiangsu Provincial Medical Youth Talent (grant number QNRC2016709).

6、 Each author contributed substantially to the study design, data acquisition, analysis and interpretation, and the writing of the manuscript. Each author gave final approval of the version to be published, and agreement to be accountable for all aspects of the work in ensuring that questions related to the accuracy or integrity of any part of the work are appropriately investigated and resolved.

7、Not applicable acknowledgement.

Table 1. The clinical data of each subtype group and inter-group differences

Parameter	A	B	C	P value (A verse B)	P value (A verse C)	P value (B verse C)
Age	56.647±9.652	59.875±12.522	58.232±10.831	0.356	0.304	0.937
Gender (female\male)	6\31	4\20	7\36	0.963	0.994	0.967
AFP (positive\negative)	32\5	11\13	30\13	0.001	0.074	0.054
ALT	64.705±65.452	116.47±105.389	68.047±77.362	0.006	0.893	0.008
AST	46.430±55.668	72.988±109.165	60.842±123.950	0.063	0.919	0.082
ALT\AST	1.55±0.79	2.070±10.96	1.504±0.752	0.092	0.728	0.044
TBIL	25.695±21.309	25.054±14.022	53.532±95.849	0.488	0.271	0.744
Direct bilirubin	13.483±12.930	12.595±9.154	28.574±50.347	0.626	0.369	0.759
Indirect bilirubin	12.208±9.239	12.463±6.494	27.284±53.889	0.425	0.191	0.724
GPC-3(positive\negative)	17\3	6\5	17\3	0.095	1	0.095

Notes: A: poorly-differentiated HCC, B: well-differentiated HCC, C: moderately-differentiated HCC, AFP: alpha fetoprotein, ALT: alamine

aminotransferase, AST: aspartate transaminase, TBIL: total bilirubin, GPC-3: glypican-3

Table 2. List of texture features extracted by MaZda software

Main features	More detailed features
Grey-level histogram	Mean, variance, skewness, kurtosis, percentiles (1%, 10%, 50%, 90%, 99%)
Grey-level co-occurrence matrix (GLCOM)	Angular second moment, contrast, correlation, entropy, sum entropy, sum of squares, sum average, sum variance, inverse difference moment, difference entropy, difference variance (for four directions and five interpixel distances (offsets; n=1-5))
Grey-level run-length matrix (GLRLM)	Run-length non-uniformity, grey-level non-uniformity, long run emphasis, short run emphasis, fraction of image in runs (for four angles)
Wavelet transform	Energies of wavelet transform coefficients in sub-bands LL, LH, HL, HH

Table 3. MRI features of each subtype group and inter-group differences

Variables	A	B	C	P value (A verse B)	P value (A verse C)	P value (B verse C)
Tumor size	7.16±7.55	4.54±3.29	4.35±3.13	0.051	0.014	0.968
Signal (Homogeneous\Heterogeneous)	12\25	14\10	18\25	0.46	0.524	0.196
Margin (Smooth\Coarse)	17\20	18\6	26\17	0.25	0.19	0.23
Capsule (Complete\Incomplete\None)	17\5\15	12\1\11	22\3\18	0.449	0.615	0.871
Liver cirrhosis (Yes\No)	20\17	12\12	23\20	0.962	0.960	0.784
HBP	7\30	7\17	8\35	0.536	0.971	0.32

hypointensity (Yes\No)						
Intra-tumoral vessel (Yes\No)	15\22	7\17	18\25	0.366	0.905	0.303
Intra-lesion fat (Yes\No)	1\36	3\21	6\37	0.327	0.168	0.867
Rim-enhancement AP (Yes\No)	22\15	12\12	15\28	0.467	0.028	0.226
lymphadenectasis (Yes\No)	5\32	1\23	1\42	0.449	0.142	1.0

Notes: A: poorly-differentiated HCC, B: well-differentiated HCC, C: moderately-differentiated HCC, Rim-enhancement AP: rim-enhancement in arterial phase.

Table 4. The frequency of each feature category extracted by FPM from AP, EP, HBP and T2 images among poorly-differentiated, well-differentiated and moderately-differentiated HCC

Texture features	A verse B	A verse C	B verse C

	AP	EP	HBP	T2	AP	EP	HBP	T2	AP	EP	HBP	T2
Histogram (n=10)	4	5	2	5	4	2	1	5	3	1	1	0
GLCOM (n=220)	15	10	17	142	14	18	19	45	16	16	19	40
GLRLM (n=20)	5	9	6	13	5	4	3	4	6	6	5	7
Wavelet transform(n=12)	6	6	5	9	7	6	7	3	5	7	5	8

Notes: A: poorly-differentiated HCC, B: well-differentiated HCC, C: moderately-differentiated HCC;
AP: arterial phase, EP: equilibrium phase images, and HBP: hepatobiliary phase.

Table 5. Misclassification rate of texture analyses from AP, EP, HBP and T2 images among poorly-differentiated, well-differentiated and moderately-differentiated HCC

	A verse B				A verse C				B verse C			
	AP	EP	HBP	T2	AP	EP	HBP	T2	AP	EP	HBP	T2
RDA (%)	44.26	34.43	50.82	48.33	55.00	50.50	47.50	46.25	34.33	46.27	44.78	47.76
PCA (%)	42.62	36.07	47.57	50.00	53.75	53.75	48.75	40.00	28.36	37.31	44.78	40.30
LDA (%)	14.75	4.92	9.84	10.00	17.50	33.75	33.75	20.00	26.87	23.88	11.94	26.87
NDA (%)	11.48	4.92	6.56	3.33	10.00	13.75	13.75	12.50	8.96	14.93	4.48	7.46

Notes: RDA, raw data analysis; PCA, principal component analysis; LDA, linear discriminant analysis; NDA, nonlinear discriminant analysis; A: poorly-differentiated HCC, B: well-differentiated HCC, C: moderately-differentiated HCC; AP: arterial phase, EP: equilibrium phase images, and HBP: hepatobiliary phase.

Table 6. The AUC of the texture features and GPC-3 among poorly-differentiated, well-differentiated and moderately-differentiated HCC

A verse B			A verse C			B verse C		
Texture features	AUC	accuracy	Texture features	AUC	accuracy	Texture features	AUC	accuracy
S(4,0)Correlat-AP	0.823	0.677	Perc.10%-AP	0.826	0.725	S(1,-1)SumAverg-AP	0.777	0.677
S(4,0)DifEntrp-EP	0.768	0.742	S(0,1)Correlat-EP	0.790	0.675	S(1,-1)SumAverg-AP+GPC-3	0.818	0.742
S(5,0)Contrast-T2	0.800	0.710	S(0,4)SumEntrp-T2	0.770	0.675			
COMBINE	0.818	0.810	135dr_RLNonUni-HBP	0.740	0.650			
COMBINE+GPC-3	0.868	0.742	COMBINE	0.880	0.800			
			COMBINE+GPC-3	0.880	0.800			

Notes: A: poorly-differentiated HCC, B: well-differentiated HCC, C: moderately-differentiated HCC; AP: arterial phase, EP: equilibrium phase images, and HBP: hepatobiliary phase. COMBINE: demonstrates the AUC of the combination of statistically significant texture features derived from different phase of Gd-EOB-DTPA-enhanced MRI.

References:

1. Ferlay J, Soerjomataram I, Dikshit R, Eser S, Mathers C, Rebelo M, Parkin DM, Forman D, Bray F: **Cancer incidence and mortality worldwide: Sources, methods and major patterns in GLOBOCAN 2012**. *INT J CANCER* 2015, **136**(5):E359-E386.
2. **EASL Clinical Practice Guidelines: Management of hepatocellular carcinoma**. *J HEPATOL* 2018, **69**(1):182-236.
3. Qiang L, Huikai L, Butt K, Wang PP, Hao X: **Factors associated with disease survival after surgical resection in Chinese patients with hepatocellular carcinoma**. *WORLD J SURG* 2006, **30**(3):439-445.
4. Shah SA, Greig PD, Gallinger S, Cattral MS, Dixon E, Kim RD, Taylor BR, Grant DR, Vollmer CM: **Factors associated with early recurrence after resection for hepatocellular carcinoma and outcomes**. *J Am Coll Surg* 2006, **202**(2):275-283.
5. Nagasue N, Uchida M, Makino Y, Takemoto Y, Yamanoi A, Hayashi T, Chang YC, Kohno H, Nakamura T, Yukaya H: **Incidence and factors associated with intrahepatic recurrence following resection of hepatocellular carcinoma**. *GASTROENTEROLOGY* 1993, **105**(2):488-494.
6. Martins A, Cortez-Pinto H, Marques-Vidal P, Mendes N, Silva S, Fatela N, Gloria H, Marinho R, Tavora I, Ramalho F *et al*: **Treatment and prognostic factors in patients with hepatocellular carcinoma**. *LIVER INT* 2006, **26**(6):680-687.
7. Zhou L, Rui JA, Ye DX, Wang SB, Chen SG, Qu Q: **Edmondson-Steiner grading increases the predictive efficiency of TNM staging for long-term survival of patients with hepatocellular carcinoma after curative resection**. *WORLD J SURG* 2008, **32**(8):1748-1756.
8. Roayaie S, Schwartz JD, Sung MW, Emre SH, Miller CM, Gondolesi GE, Krieger NR, Schwartz ME: **Recurrence of hepatocellular carcinoma after liver transplant: patterns and prognosis**. *Liver Transpl* 2004, **10**(4):534-540.
9. Tamura S, Kato T, Berho M, Misiakos EP, O'Brien C, Reddy KR, Nery JR, Burke GW, Schiff ER, Miller J *et al*: **Impact of histological grade of hepatocellular carcinoma on the outcome of liver transplantation**. *Arch Surg* 2001, **136**(1):25-30, 31.
10. Huang K, Dong Z, Cai H, Huang M, Peng Z, Xu L, Jia Y, Song C, Li ZP, Feng ST: **Imaging biomarkers for well and moderate hepatocellular carcinoma: preoperative magnetic resonance image and histopathological correlation**. *BMC CANCER* 2019, **19**(1):364.
11. Stigliano R, Burroughs AK: **Should we biopsy each liver mass suspicious for HCC before liver transplantation?--no, please don't**. *J HEPATOL* 2005, **43**(4):563-568.
12. Stigliano R, Marelli L, Yu D, Davies N, Patch D, Burroughs AK: **Seeding following percutaneous diagnostic and therapeutic approaches for hepatocellular carcinoma. What is the risk and the outcome? Seeding risk for percutaneous approach of HCC**. *CANCER TREAT REV* 2007, **33**(5):437-447.

13. Kogita S, Imai Y, Okada M, Kim T, Onishi H, Takamura M, Fukuda K, Igura T, Sawai Y, Morimoto O *et al*: **Gd-EOB-DTPA-enhanced magnetic resonance images of hepatocellular carcinoma: correlation with histological grading and portal blood flow**. *EUR RADIOL* 2010, **20**(10):2405-2413.

14. Nishie A, Yoshimitsu K, Okamoto D, Tajima T, Asayama Y, Ishigami K, Kakihara D, Nakayama T, Takayama Y, Shirabe K *et al*: **CT prediction of histological grade of hypervascular hepatocellular carcinoma: utility of the portal phase**. *JPN J RADIOL* 2013, **31**(2):89-98.

15. Kaseb AO, Hassan M, Lacin S, Abdel-Wahab R, Amin HM, Shalaby A, Wolff RA, Yao J, Rashid A, Vennapusa B *et al*: **Evaluating clinical and prognostic implications of Glypican-3 in hepatocellular carcinoma**. *ONCOTARGET* 2016, **7**(43):69916-69926.

16. Ho M, Kim H: **Glypican-3: A new target for cancer immunotherapy**. *EUR J CANCER* 2011, **47**(3):333-338.

17. Feng J, Zhu R, Chang C, Yu L, Cao F, Zhu G, Chen F, Xia H, Lv F, Zhang S *et al*: **CK19 and Glypican 3 Expression Profiling in the Prognostic Indication for Patients with HCC after Surgical Resection**. *PLOS ONE* 2016, **11**(e01515013).

18. Yamauchi N, Watanabe A, Hishinuma M, Ohashi K, Midorikawa Y, Morishita Y, Niki T, Shibahara J, Mori M, Makuuchi M *et al*: **The glypican 3 oncofetal protein is a promising diagnostic marker for hepatocellular carcinoma**. *MODERN PATHOL* 2005, **18**(12):1591-1598.

19. Castellano G, Bonilha L, Li LM, Cendes F: **Texture analysis of medical images**. *CLIN RADIOL* 2004, **59**(12):1061-1069.

20. Scalco E, Rizzo G: **Texture analysis of medical images for radiotherapy applications**. *Br J Radiol* 2017, **90**(1070):20160642.

21. Eun NL, Kang D, Son EJ, Park JS, Youk JH, Kim JA, Gweon HM: **Texture Analysis with 3.0-T MRI for Association of Response to Neoadjuvant Chemotherapy in Breast Cancer**. *RADIOLOGY* 2019:182718.

22. Colakoglu B, Alis D, Yergin M: **Diagnostic Value of Machine Learning-Based Quantitative Texture Analysis in Differentiating Benign and Malignant Thyroid Nodules**. *J ONCOL* 2019, **2019**:6328329.

23. Kielar AZ, Chernyak V, Bashir MR, Do RK, Fowler KJ, Mitchell DG, Cerny M, Elsayes KM, Santillan C, Kamaya A *et al*: **LI-RADS 2017: An update**. *J MAGN RESON IMAGING* 2018, **47**(6):1459-1474.

24. Szczypinski PM, Strzelecki M, Materka A, Klepaczko A: **MaZda--a software package for image texture analysis**. *Comput Methods Programs Biomed* 2009, **94**(1):66-76.

25. Yan L, Liu Z, Wang G, Huang Y, Liu Y, Yu Y, Liang C: **Angiomyolipoma with minimal fat: differentiation from clear cell renal cell carcinoma and papillary renal cell carcinoma by texture analysis on CT images**. *ACAD RADIOL* 2015, **22**(9):1115-1121.

26. Lee JH, Lee JM, Kim SJ, Baek JH, Yun SH, Kim KW, Han JK, Choi BI: **Enhancement patterns of hepatocellular carcinomas on multiphasic multidetector row CT: comparison with pathological differentiation**. *BRIT J RADIOL* 2012, **85**(1017):E573-E583.

27. Chen WT, Chau GY, Lui WY, Tsay SH, King KL, Loong CC, Wu CW: **Recurrent hepatocellular carcinoma after hepatic resection: prognostic factors and**

long-term outcome. *EJSO-EUR J SURG ONC* 2004, **30**(4):414-420.

28. Holli-Helenius K, Salminen A, Rinta-Kiikka I, Koskivuo I, Bruck N, Bostrom P, Parkkola R: **MRI texture analysis in differentiating luminal A and luminal B breast cancer molecular subtypes - a feasibility study**. *BMC MED IMAGING* 2017, **17**(1):69.

29. Gillies RJ, Kinahan PE, Hricak H: **Radiomics: Images Are More than Pictures, They Are Data**. *RADIOLOGY* 2016, **278**(2):563-577.

30. Mule S, Thiefin G, Costentin C, Durot C, Rahmouni A, Luciani A, Hoeffel C: **Advanced Hepatocellular Carcinoma: Pretreatment Contrast-enhanced CT Texture Parameters as Predictive Biomarkers of Survival in Patients Treated with Sorafenib**. *RADIOLOGY* 2018, **288**(2):445-455.

31. Li Y, Yan C, Weng S, Shi Z, Sun H, Chen J, Xu X, Ye R, Hong J: **Texture analysis of multi-phase MRI images to detect expression of Ki67 in hepatocellular carcinoma**. *CLIN RADIOL* 2019, **74**(10):813-819.

32. Lubner MG, Smith AD, Sandrasegaran K, Sahani DV, Pickhardt PJ: **CT Texture Analysis: Definitions, Applications, Biologic Correlates, and Challenges**. *RADIOGRAPHICS* 2017, **37**(5):1304-1483.

33. Zhou W, Zhang L, Wang K, Chen S, Wang G, Liu Z, Liang C: **Malignancy Characterization of Hepatocellular Carcinomas Based on Texture Analysis of Contrast-Enhanced MR Images**. *J MAGN RESON IMAGING* 2017, **45**(5):1476-1484.

34. Kandil DH, Cooper K: **Glypican-3 A Novel Diagnostic Marker for Hepatocellular Carcinoma and More**. *ADV ANAT PATHOL* 2009, **16**(2):125-129.

35. Yorita K, Takahashi N, Takai H, Kato A, Suzuki M, Ishiguro T, Ohtomo T, Nagaike K, Kondo K, Chijiiwa K *et al*: **Prognostic significance of circumferential cell surface immunoreactivity of glypican-3 in hepatocellular carcinoma**. *LIVER INT* 2011, **31**(1):120-131.

Figures

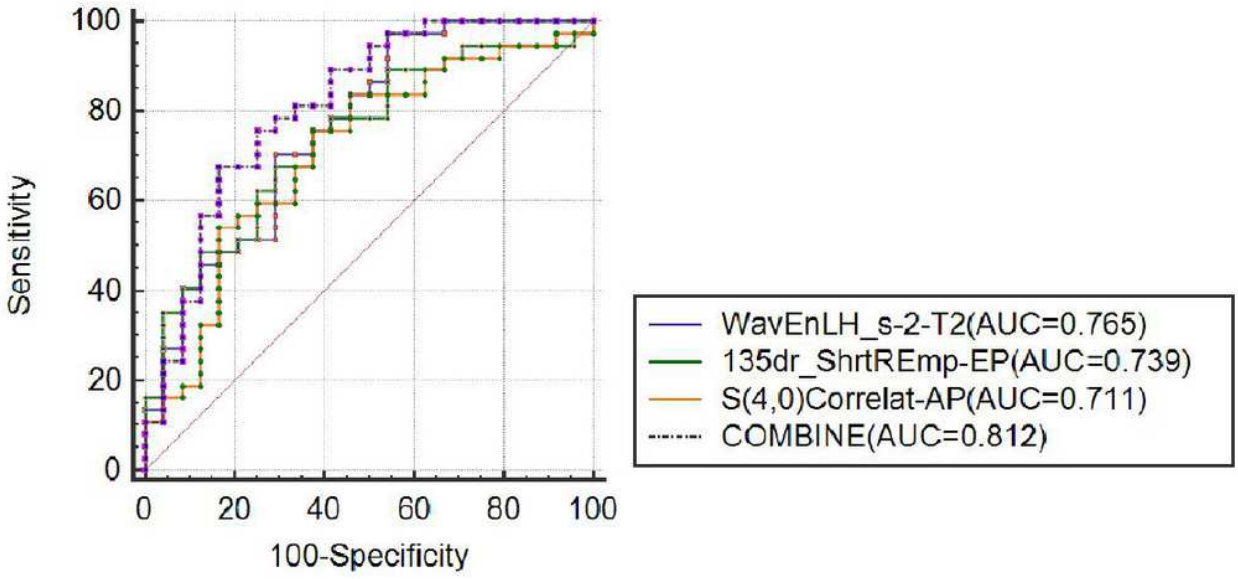

Figure 1

ROC for differentiating the poorly- and well-differentiated HCC. The ROC curves were draw according to the texture features with the highest AUC derived from T2, EP and AP. And the ROC of the combined texture features was also draw as COMBINE.

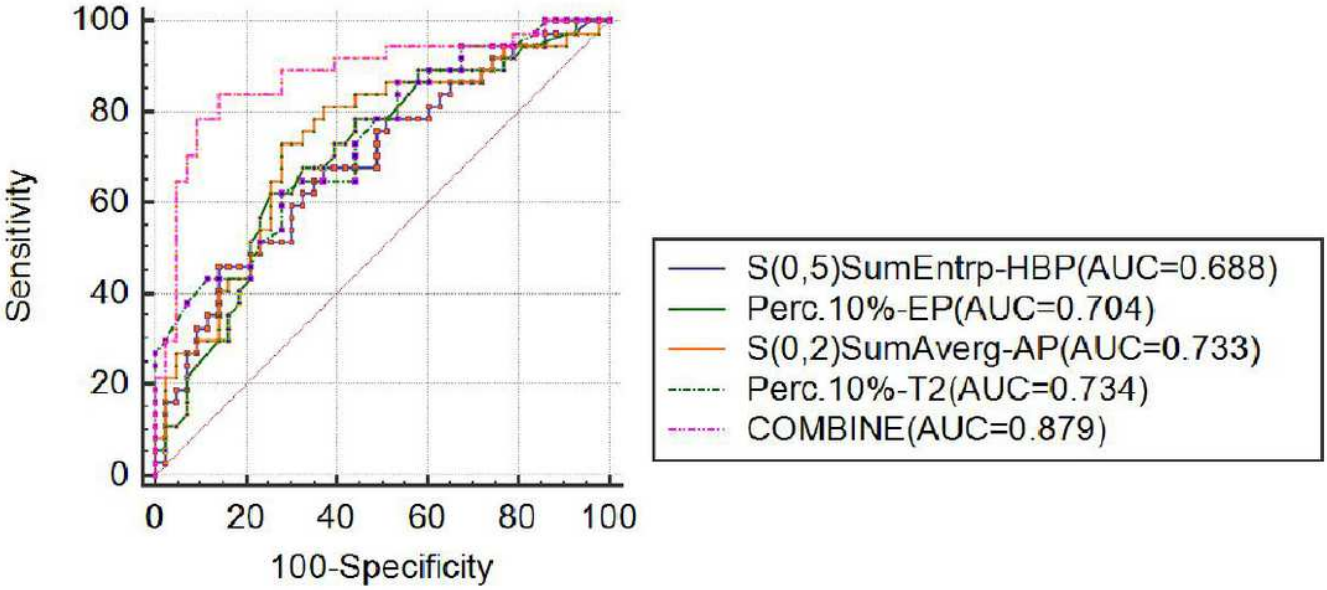

Figure 2

ROC for differentiating the poorly- and moderately-differentiated HCC. The ROC curves were draw according to the texture features with the highest AUC derived from T2, AP, EP and HBP. And the ROC of the combined texture features was also draw as Combine.

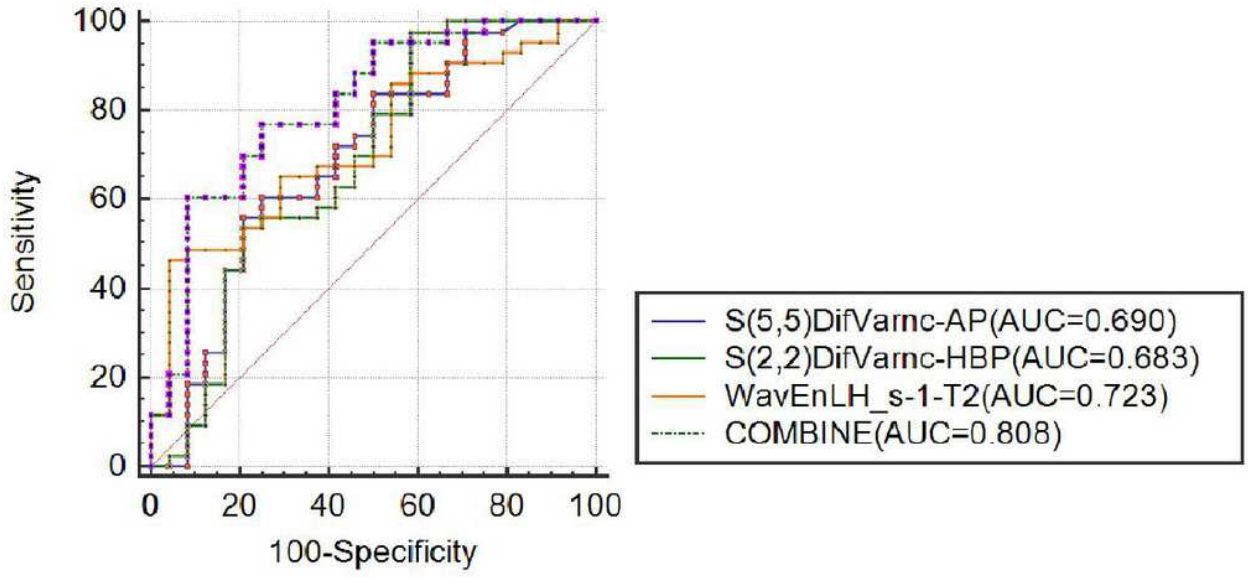

Figure 3

ROC for differentiating the well- and moderately-differentiated HCC. The ROC curves were draw according to the texture features with the highest AUC derived from T2, AP and HBP. And the ROC of the combined texture features was also draw as Combine.